Trakia Journal of Sciences, Vol. 8, Suppl. 2, pp 84-91, 2010

Available online at:
http://www.uni-sz.bg

**ISSN 1313-7050 (print)**
**ISSN 1313-3551 (online)**

# SOME THEORETICAL CONSIDERATIONS ABOUT POSSIBILITY OF LIMITATION OF ESWL PROCEDURE INJURES

**Iv. Antonov***

Department of Medical Physics and Biophysics, Medical University, Sofia

**ABSTRACT**
The underlying principle of ESWL is the creation of a shock wave by an energy source which is targeted using a focusing device, and the energy is then conveyed from outside to inside the body via a coupling mechanism, usually a fluid medium. The number of shock waves and treatments needed for breakage of stones depends upon their size and hardness. Numerous experimental investigations confirm that the physics of the secondary destructive mechanism is directly related to the wide spectrum of phenomena studied within the frame work of medical applications of shock-wave and ultrasonic diagnostics for special aims. Micro bubbles and cavitation clusters, their interaction with shock waves (SW) and SW generation, micro bubble pulsations and cumulative micro jets play both the positive a kidney stone disintegration by ESWL (SW) and undesirable (destruction of tissues and cells) roles in the processes of damage, destroying and treatment. The effect of rarefaction phases of ESWL shock waves as well as its focusing on the target as one of elements of the mechanism of kidney stone destruction will be discussed. And as the preface the short survey of some biomedical problems will be presented to show the important role of SW and bubble clusters in their solution.

**Key words:** Kidney stones · Injury · Cavitation · Shock wave

## FUNDAMENTALS OF SHOCK VAWE PROPAGATION

A simple shock vawe (SW) is a plane steady shock propagating in a semi-infinity medium. It can be generated by applying normal stress on the surface of a half-space as illustrated in **Fig. 1** In this figure SW moves left to right with the velocity ***U*** relative to stationary laboratory coordinates.

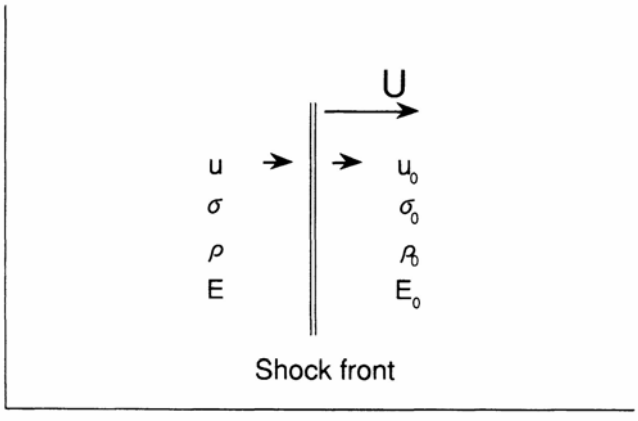


**Figure 1.** A schematic representation of an idealized shock wave in an infinite medium.

***Correspondence to:** *Ivan Georgiev Antonov, Department of Medical Physics and Biophysics, Medical University, 2 Zdrave Str., Sofia 1431, email: ivanantonov@abv.bg*

The nature of the discontinuity can be studied by applying the conservation of mass, linear momentum, and energy to a unit cross-sectional area of the flowing material relative to the observer who moves with the shock

front. According this suggestion we may write general relationships between mass flux per unit area (***m***), linear momentum per unit time (***σ***-compressive stress normal to the front), and change in internal energy (***E***) of the system observed at the front:

$$\rho(u-U)=\rho_0(u_0-U)=m \tag{1.1}$$

$$\sigma-\sigma_0=m(u-u_0) \tag{1.2}$$

$$\sigma(u-U)-\sigma_0(u_0-U)=m\left[\frac{1}{2}(u_0-U)^2-\frac{1}{2}(u-U)^2+(E_0-E)\right] \tag{1.3}$$

It is clear from Eqs (1.1)-(1.3) that if a supplementary relationships between $\sigma$, medium density $\rho$, and energy $E$ are known (from experiment), these equations define a unique curve in the ***σ-ρ*** plane representing states that are attainable by a single jump from a particular initial state. In the case of a fluid, ***σ*** becomes the hydrodynamic pressure $p$, and use the substitution $V=1/\rho$- (specific volume) we obtained parametric relationships $p=f(V)$, so called a Hugeniot [1] curve **Fig. 2.**

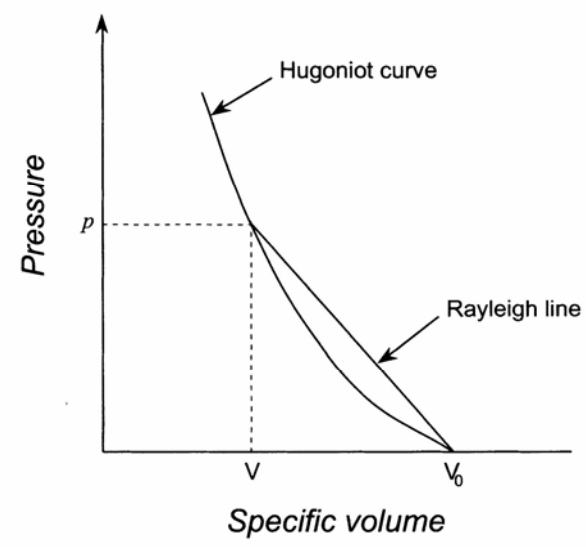


**Figure 2.** A schematic Hugoniot curve.

The chord drawn from the initial state to state $p$, called Rayleigt line, defines the shock velocity through the relationship

$$-U^2=V_0^2\frac{\Delta p}{\Delta V}, \tag{1.4}$$

where **Δ** signifies the discontinues changes in $p$ and $V$.

The particle velocity (***u***) relative to material ahead the shock is given:

$$u=\left[(\sigma-\sigma_0)(V_0-V)\right]^{\frac{1}{2}} \tag{1.5}$$

For a single shock starting at zero pressure, it may be deducted from Eqs.(1.3) that the energy imparted by the shock is equally partitioned between internal and kinetic energy.(per unit mass):

$$E=\frac{1}{2}p(V_0-V)=\frac{1}{2}u^2 \tag{1.6}$$

To obtain information about dissipative possesses like at plastic deformation, viscosity dissipation, we start with derivative of Eqs.(1.6) and second low of thermodynamic. Expanding the entropy in terms of specific volume and pressure one finds,

$$\begin{aligned} dE&=\frac{dp}{2}(V_0-V)-\frac{p}{2}dV \\ dE&=TdS-pdV \\ dS&=\left(\frac{\partial S}{\partial p}\right)_V dp+\left(\frac{\partial S}{\partial V}\right)_p dV \end{aligned}, \tag{1.7}$$

where ***S*** signifies the entropy. Now eliminates ***dE*** and ***dS*** from Eqs.(1.7), after some simplification, one obtains the differential equation for Hugeniot curves,

$$\frac{dp}{dV} = \frac{\left(\frac{\partial p}{\partial V}\right)_S + \gamma \frac{p}{2V}}{1 - \gamma \frac{(V_0 - V)}{2V}}, \qquad (1.8)$$

where $\gamma$ is given by

$$\gamma = \frac{V}{C_V}\left(\frac{dp}{dT}\right)_V, \qquad (1.9)$$

and $C_V$ is the specific head at constant volume.

## THEORETICAL AND EXPERIMENTAL RESULTS FOR SW– KIDNEY STONES INTERACTION

In an ESWL treatment the urologist controls three parameters: the number of shock waves administered, the repetition rate, and the voltage (or energy) of the shock wave generator. The latter is directly associated to the amplitude of the pressure wave. Typically, from one to three thousand shock waves are fired onto the stone at a rate of around one per second. A very important factor in the treatment is the lithotripter device, because it determines the profile of the ESWL impulse. The most common lithotripters are electro-hydraulic devices, e.g., the Dornier HM3, which generate shock waves by underwater spark discharge. The waves are focused by a brass ellipsoidal reflector to an area of approximately 10–15mm in diameter and with peak pressures in the range of 30–50MPa. A typical pressure measurement at the focus of a HM3 lithotripter is shown in **Fig. 3a**. A narrow positive pressure spike with short rise time and rapid fall (<1ms) is followed by a significant negative pressure, the so called "tension tail".

An analytical expression (often used in numerical models) of such an ESWL impulse was given in Howle et al. [2] **Fig. 3b**:

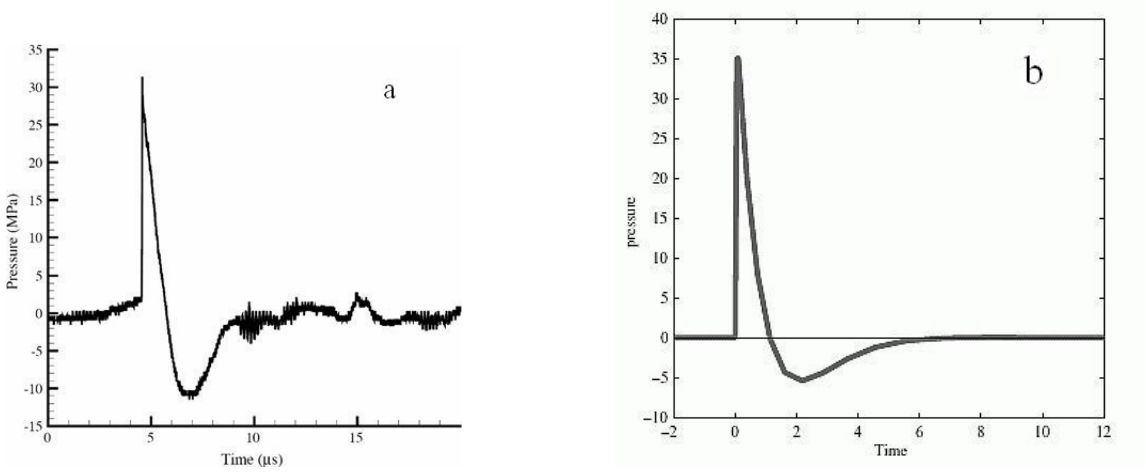


**Figure 3.** Experimentally measured ESWL impulse at the focal point of a HM3 lithotripter (a) and impulse after Eqs. (2.1) (b).

$$p(t) = \begin{cases} 2p_{\max} \exp\left(\frac{-t}{\tau_1}\right)\cos\left(\frac{t}{\tau_2} + \frac{\pi}{3}\right) & \text{if } 0 \le t \le \frac{7\pi}{6}\tau_2 \\ 0 \qquad \text{otherwise} \end{cases} \qquad (2.1)$$

The time variables $\tau_1$ and $\tau_2$ determines the profile of the ESWL impulse, $\tau_1$ characterizes the pressure decay and $\tau_2$ the duration. The exact mechanisms of stone breakage are still a topic of debate, but two mechanisms have been substantiated by empirical observation:

***Spallation*** is a material failure caused by tensile stress. Tension is induced as the compressive part of the pressure wave is reflected by the distal stone–tissue interface as a tensile wave. The reflected wave combines with the tensile tail of the incident wave to produce a plane of maximum tensile stress that can cleave the stone. Using the basic Eqs.(1.1-1.4) from previous section, in case of spherical symmetry, we obtain the parametrical relationships about time and spatial distribution for a single SW:

$$E(t)=\int_0^{r(t)}\left\{\frac{p(t)}{\gamma-1}-\frac{\rho(t)u^2}{2}\right\}4\pi r(t)dr$$

$$p(t)=\frac{8}{25}\frac{k^2\rho_0}{\gamma+1}\left(\frac{E}{\rho_0}\right)^{\frac{2}{5}}t^{-\frac{6}{5}} \qquad (2.2)$$

$$r(t)=k\left(\frac{E}{\rho_0}\right)^{\frac{1}{5}}t^{-\frac{2}{5}}$$

In the upper expressions $k$ is constant, which value depend only of solution of Eqs.(1.9). A typical form of SW obtained from upper solution and Eqs.(2.1), in case $\tau_2$=1ms., $\tau_1$=10ms.,$p_{max}$=50MPa and $\gamma$=(1.004 -water) is shown in **Fig. 4**. The *x*-axis and *r*-axis showing normal and radial distribution of pressure after time interval *t*=100ms. In such figure well see the "tail" of the SW - negative pressure component. The tensile stress is:

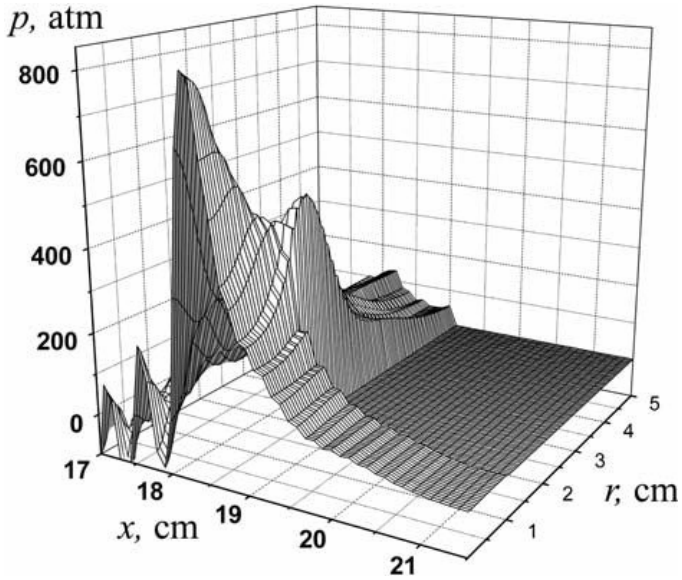


**Figure 4.** Solitary shock wave. Spatial distribution of pressure in case of spherical simetry.

$$\sigma(t)=\Delta p_{1,2}(t)$$

$$p_1(t)=\frac{\pi^{\frac{1}{2}}}{2r(t)}\sqrt{Z_1\left(\frac{\partial\xi_1}{\partial r}\right)\frac{\partial E}{\partial t}}, \qquad p_2(t)=\frac{\pi^{\frac{1}{2}}}{2r(t)}\sqrt{Z_2\left(\frac{\partial\xi_2}{\partial r}\right)\frac{\partial E}{\partial t}} \qquad (2.3)$$

where $Z$ signified acoustic impedance of the media and $\xi$ is tensile modulus for this point. In general, the values of latter are complicate function (see Eqs.(2.2)) from energy and *r*.

***Erosion*** is caused by the action of cavitating bubbles near the stone. The tensile wave component typically generates bubbles (or clouds of bubbles) that oscillate in size and collapse violently after the passage of the wave [5,6].

In contrast to the fracture in solids, pulse loading in liquids does not involve a stage at which fracture centers develop. The macroscopic structure of the liquid is such that even when the liquid is carefully purified by distillation or deionization there are always microinhomogeneities, which act as cavitation nuclei. These can be microbubbles of free gas, solid particles, or their conglomerates **(Fig. 5a)**. F**igure 5b** shows the probable size distribution of microinhomogeneities based on the results of Hammitt et al. (dots) [7] averaged over a wide spread of experimental data, Strasberg's results (crosses) [8], and those obtained in the Kedrinskii [9]. Determination of the nature of these microinhomogeneities, their parameters, density, and size spectra are the basic problems of the analysis of the state of a real liquid.

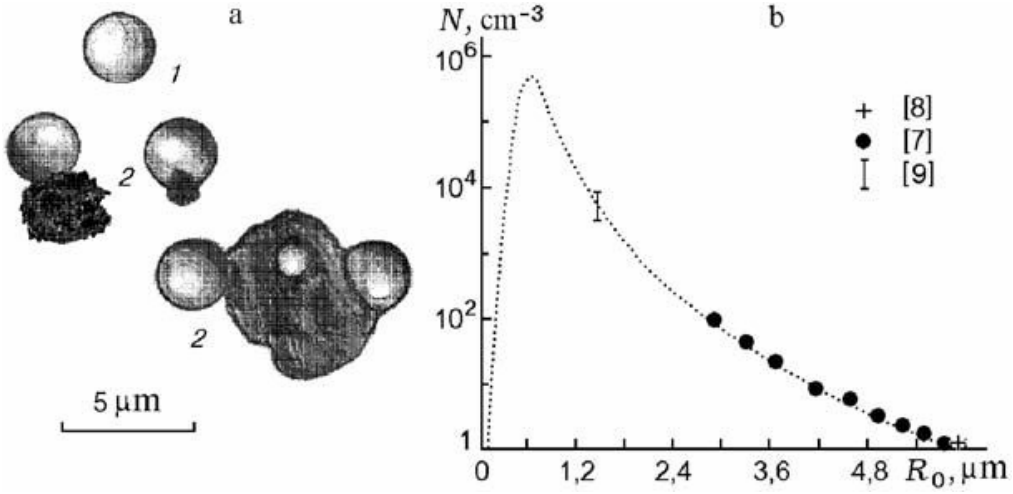


**Figure 5.** The structure of microinhomogeneities (a) and the spectrum of cavitation nuclei (b): (1) free gas bubbles and (2) combination structures.

According to the results from the model experiment by Besov [10], the disintegration process consisted of two stages. A dense cavitation zone formed at the initial stage **(Fig. 6)**. The first frame shows the initial state: the drop is transparent and through it one can clearly see the surface structure of the duralumin membrane. The impact of the diaphragm on the drop (diameters of drop was about 2 cm, of membrane was 8 cm) produced a circular cumulative jet as a thin veil and the first microclusters of cavitation bubbles of millimeter size (**Fig. 6**, frame 2). The structure of the cavitation zone was determined by the increasing number of macroclusters apparently formed during the growth of microinhomogeneities and their fusion. To 70 μs the drop "boils up" (Fig. 6, frame 4) acquiring a distinct honeycomb structure. Then the cavitation zone is developing by inertia and the drop is transforming into a spatial grid with clear zones as cells of liquid bunches **(Fig. 6b**), wherein the main mass of the initial drop was probably concentrated. The elements of the liquid grid under further stretching were gradually separated into individual fragments, small jets, which due to instability disintegrated into individual drops. It is noteworthy that even in the droplet state the flow retained the cellular pattern of the structure over a long time. Thus, the cavitation zone generated by strong rarefaction wave was a system of bubble microclusters formed at the initial stage of expansion and integration of cavitation nuclei. The inertial development of these microclusters led to the formation of a dome as a honeycomb structure of the type of a liquid grid with a thin film. The disintegration of the grid cells into individual jets and then into droplets (**Fig. 6c**) formed the basis of the inversion mechanism of the two-phase state (foam-droplet transition) under dynamic loading of a liquid [11].

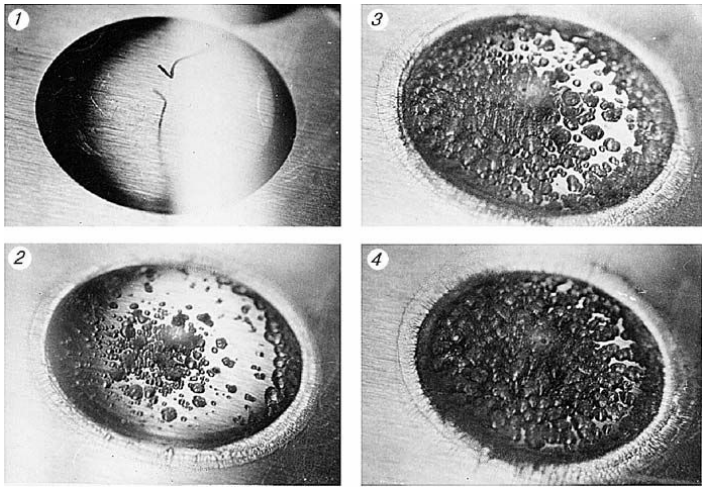


**Figure 6.** Formation of the system of bubble clusters in a drop loaded by an ultrashort shock wave.

It should be noted that the rough surface of the target in which protrusions may alternate with depressions favors the disintegration, following the mechanism proposed by Field et al. [12] to explain the surface erosion under the impact of liquid droplets. Indeed, according to the model, the impact and flowing of the droplet may result in formation of convergent shock waves and cumulative jets **(Fig. 7)**.

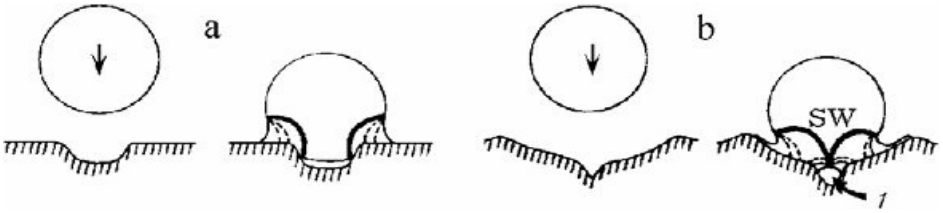


**Figure 7.** Unevenness of the target surface favors its disintegration [12] under the impact by a drop: central hollow (1) and focused shock wave (SW).

**Figure 8** shows (computer simulation by Kedrinskii, Matsumoto, [13] ) the dynamics of spatial distribution of bubble radii and pressure during focusing of the shock wave from the distance of 10 cm for the times 50, 60, and 170 μs from the onset of the process ($k_0$=10−4, $R_0$=1 mm). One can see that already after 60 μs the shock wave reached the target surface (dotted line, the target radius was 1 cm). Its parameters were close to those mentioned in [14], including the rather long rarefaction phase with an amplitude of several MPa. The distribution of bubble radii by that time showed no peculiarities: they collapsed intensely under the effect of the shock wave near the target and their radius was somewhat greater at the periphery (the boundary of "launching" of the shock wave toward the cylindrical target).

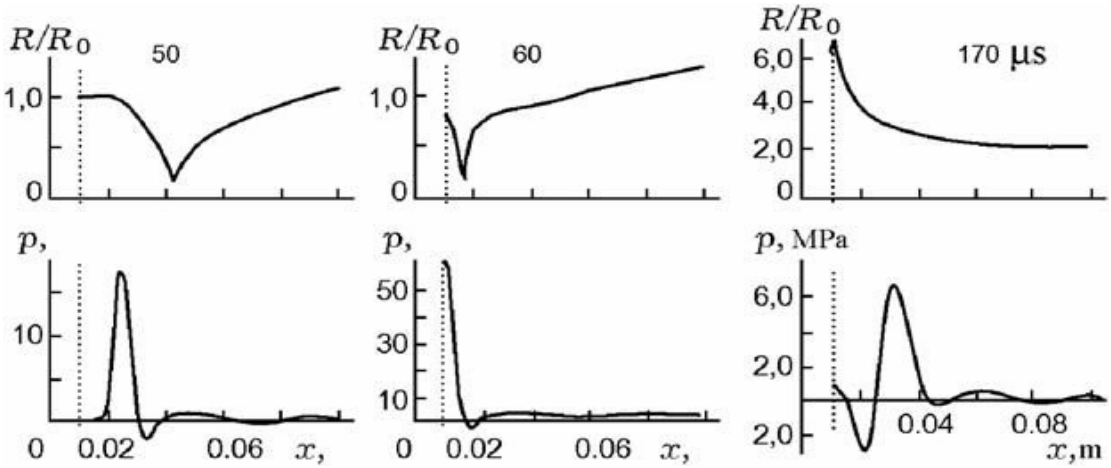


**Figure 8.** Development of the cavitation zone near the focus (relative change of the bubble radius $R/R_0$ in the zone) and the dynamics of the shock wave profile.

After 170 μs the situation changed considerably: as a result of reflection a dense bubble cluster (about 1–2 cm thick) was formed on the target. By this time, the volume concentration $k$ in the cluster increases by about a factor of 300 and pressure in the bubbles was almost zero. One could expect that according to the above experimental and theoretical data the pressure difference at the external boundary of the bubble cluster and the mean pressure inside it should lead to the cluster collapse and the mentioned hydraulic effect.

A well, "real time" demonstration, of the mentioned mechanisms was given by Delius in [15]. **Figure 9** presents three intervals (1–3) of the formation of a bubble cluster on the stone surface under shock-wave focusing (Delius' experiments, 1990).The time between frames in each interval was 40 μs and the time lag between successive intervals was 200 μs. The shock wave was generated by Dornier Lithotriptor with the amplitude of 65 MPa in the front and a rarefaction phase of maximum amplitude −6 MPa. A stone was positioned onto a metal foil in the geometrical focus of the lithotriptor.

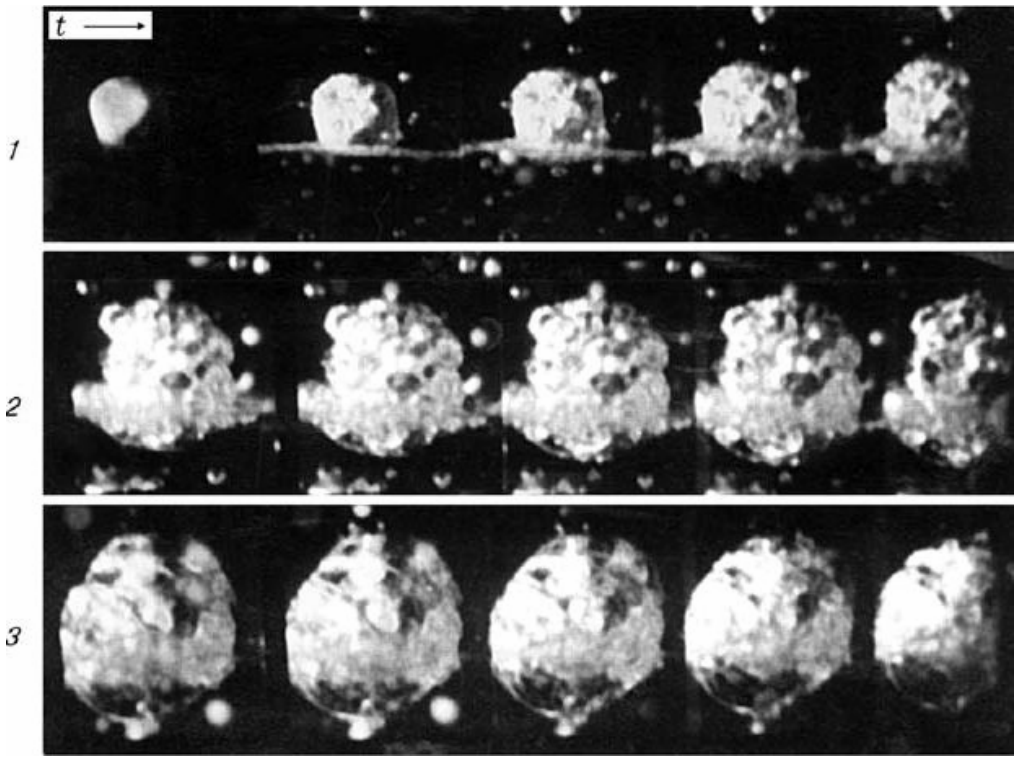


**Figure 9.** Formation of a bubble cluster formation on the stone surface [15]

**CONCLUSION**

It's well known that lithotripsy is a common effective treatment for kidney stones. However, focal volumes are often larger than stones, and surrounding tissue is often injured. Delius [15] considered three possible mechanisms of tissue damage by shock waves: thermal effect, direct mechanical effect, and the indirect effect called cavitation. His estimates showed that for typical wave forms generated in the systems one can expect a temperature decrease by about 2 ◦C for a pulse frequency of 100 Hz. Delius related the damage to the formation of cumulative microjets produced either by asymmetrical collapse of the bubble near the target solid wall or by the interaction of the cavitation bubble with the shock wave.[16] Similar effects were observed by Kitayama et al. [17], who noted that after the wave focusing, pressure around the target reduces sharply, which leads to the formation of a cavitation zone. It is assumed that over this time cracks grow around the stone, then they are widened to a certain maximum size, and finally a collapse occurs. Grunevald et al. [18] proposed an acoustic scheme for calculating the pressure field in the shock wave focus that takes into account the shift of the source.

Sokolov, Bailey and Crum [19] have suggested new dual-pulse lithotripter consisting of two opposing, confocal and simultaneously triggered electrohydraulic sources to accelerate stone fragmentation and to reduce cell lysis in vitro. Model gypsum stones and human erythrocytes were exposed to dual pulses or single pulses. The results of tests in vitro have shown that at the focus, model stones treated with 100 dual pulses at a charging voltage of 15 kV broke into eight times the number of fragments as stones treated with 200 single pulses at 18 kV.

Often for the study of these phenomena it's required to determine the special (including 3D) mathematical models. With this point of view the results published in [17-20] become interesting. Summarizing existing today numerical models of ESWL, it may to say that it's a powerful tool for studying the effect of shock waves on soft tissue. With detailed finite-element models of the kidney that maps the various structures individually and accounts for inelastic strain, cavitation and volume expansion it's able to predict the onset of damage in the kidney tissue. These results compare well with medical and experimental findings. In particular, the some models are able to analyze the influence of form and energy of the ESWL

impulse on the tissue [20]. The authors findings suggest that not the initial compressive pressure front of the shock wave induces tissue damage but rather the greater tensile stress caused by the tail of the impulse. Therefore, comparing two ESWL impulses with same energy transport the one with larger tensile amplitude is more destructive. Nonetheless, the same models approach provides an efficient strategy to limited side effects of shock-wave lithotripsy treatments.

**REFERENCES**


1. Plagemann M (2006) Numerische Untersuchungen zur Belastung der menschlichen Niere während einer Lithotripsie-Behandlung. Studienarbeit, Institut für Mechanik, TU Berlin
2. Howle L, Schaefer DG, Shearer M, Zhong P (1998) Lithotripsy: the treatment of kidney stones with shock waves. SIAM 40: pp. 356–371
3. Simo JC, Hughes TJR (1998) Computational inelasticity. Springer, Berlin
4. B.I. Zaslavskii: On Reflection of Spherical Shock Wave in Water from Free Surface, Zh. Prikl. Mekh. i Tekh. Fiz. **4**, 6, pp. 50–59 (1963)
5. Nasseri S, Bilston LE, Phan-Thien N (2002) Viscoelastic properties of pig kidney in shear, experimental results and modelling. Rheol Acta 41: pp.180–192
6. Sturtevant B, LokhandwallaM (1998) Biomechanical effects of ESWL shock waves. J Acoust Soc Am 103: pp. 3037–3053
7. Howle L, Schaefer DG, Shearer M, Zhong P (1998) Lithotripsy: the treatment of kidney stones with shock waves. SIAM 40: pp. 356–371
8. F.G. Hammitt, A. Koller, O. Ahmed, J. Pjun, E. Yilmaz: Cavitation threshold and superheat in various fluids. In: Proc. of Conf. on Cavitation (Mech. Eng. Publ. Ltd, London, 1976), pp. 341–354
9. M. Strasberg: Undissolved air cavities as cavitation nuclei. In: Cavitation in Hydrodynamics (National Phys. Lab., London, 1956)
10. A.S. Besov, V.K. Kedrinskii, E. I. Pal'chikov: Studying of Initial Stage of Cavitation Using Diffraction-Optic Method, Pis'ma Zh. Exp. Teor. Fiz. **10**, 4, pp. 240–244 (1984)
11. A. Besov, V. Kedrinskii: Dynamics of bubbly clusters and free surface at shock wave reflection. In: J. Blake, J. Boulton-Stone, N. Thomas (eds.) Proc. Intern. Symp. on Bubble Dynamics and Interface Phenomena (Birmingham, 6–9 Sept. 1993, Kluwer Academic Publisher, 1994), pp. 93–103
12. J.E. Field, M.B. Lesser, J.P. Dear: Proc. Roy. Soc. London **A**, 401 (1985)
13. A.S. Besov, V.K. Kedrinskii, Y. Matsumoto et al.: Microinhomogeneity structures and hysteresis effects in cavitating liquids. In: Proc. 14th Int. Congress on Acoustics (Beijing, 1992), pp. 1–3 T.
14. Okada, Y. Iwai, Y. Hosokawa: Comparison of Surface Damage Caused by Sliding Wear and Cavitation Erosion on Mechanical Face Seal, J. Tribology, 42 (1984)
15. M. Delius: Zentralblatt f¨ur Chirurgie, **120**, 4 (1995) pp. 259–273
16. M. Delius, F. Ueberle, W. Eisenmenger: Ultrasound in Medicine and Biology **24**, 7 (1998) pp. 1055–1059
17. O. Kitayama, H. Ise, T. Sato, K. Takayama: Non-invasive gallstone disintegration by underwater shock focusing. In: H. Gr¨onig (ed.) Proc. 16th Intern. Symp. on Shock Tubes and Waves (VCH, Aachen, 1987) pp. 897–904
18. M. Grunevald, H. Koch, H. Hermeking: Modeling of shock wave propagation and tissue interaction during ESWL. In: H. Gr¨onig (ed.) Proc. 16th Intern. Symp. on Shock Tubes and Waves (VCH, Aachen, 1987) pp. 889–895
19. D.L. Sokolov, M.R. Bailey, L.A. Crum: Ultrasound in Medicine and Biology, **29**, 7 (2003) pp. 1045–1052
20. K. Weilberg, M.Ortis Kidney damage in extracorporeal shock wave lithotripsy:a numerical approach for different shock profiles. Springer, Biomeh Model Mechanobiol (2009) **8**: pp. 285-299